

## Precise Characterization of ${}^6\text{Li}$ Feshbach Resonances Using Trap-Sideband-Resolved RF Spectroscopy of Weakly Bound Molecules

G. Zürn,<sup>1,2</sup> T. Lompe,<sup>1,2,3,\*</sup> A. N. Wenz,<sup>1,2</sup> S. Jochim,<sup>1,2,3</sup> P. S. Julienne,<sup>4</sup> and J. M. Hutson<sup>5,†</sup>

<sup>1</sup>Physikalisches Institut, Ruprecht-Karls-Universität Heidelberg, 69120 Heidelberg, Germany

<sup>2</sup>Max-Planck-Institut für Kernphysik, Saupfercheckweg 1, 69117 Heidelberg, Germany

<sup>3</sup>ExtreMe Matter Institute EMMI, GSI Helmholtzzentrum für Schwerionenforschung, 64291 Darmstadt, Germany

<sup>4</sup>Joint Quantum Institute, NIST and the University of Maryland, Gaithersburg, Maryland 20899-8423, USA

<sup>5</sup>Department of Chemistry, Joint Quantum Centre (JQC) Durham/Newcastle, Durham University, South Road, Durham DH1 3LE, United Kingdom

(Received 6 November 2012; published 25 March 2013)

We perform radio-frequency dissociation spectroscopy of weakly bound  ${}^6\text{Li}_2$  Feshbach molecules using low-density samples of about 30 molecules in an optical dipole trap. Combined with a high magnetic field stability, this allows us to resolve the discrete trap levels in the radio-frequency dissociation spectra. This novel technique allows the binding energy of Feshbach molecules to be determined with unprecedented precision. We use these measurements as an input for a fit to the  ${}^6\text{Li}$  scattering potential using coupled-channel calculations. From this new potential, we determine the pole positions of the broad  ${}^6\text{Li}$  Feshbach resonances with an accuracy better than  $7 \times 10^{-4}$  of the resonance widths. This eliminates the dominant uncertainty for current precision measurements of the equation of state of strongly interacting Fermi gases. As an important consequence, our results imply a corrected value for the Bertsch parameter  $\xi$  measured by Ku *et al.* [*Science* **335**, 563 (2012)], which is  $\xi = 0.370(5)(8)$ .

DOI: [10.1103/PhysRevLett.110.135301](https://doi.org/10.1103/PhysRevLett.110.135301)

PACS numbers: 67.85.-d

In the past few years, ultracold Fermi gases of neutral atoms have become important benchmark systems for testing theories of strongly interacting many-body systems [1]. This success is based on two main factors. The first is that the physics of ultracold gases is very well approximated by simple model Hamiltonians. These Hamiltonians contain only a contact interaction, which can be described by a single quantity: the scattering length  $a$ . The second is the existence of Feshbach resonances in the interparticle scattering, which cause the scattering length to diverge to  $\pm\infty$  at certain magnetic field values  $B_0$  [2]. This allows tuning of the interparticle interactions by applying a homogeneous magnetic offset field. Using such resonances, the properties of strongly interacting Fermi gases have been investigated using a number of different techniques, which range from radio-frequency (RF) spectroscopy [3,4], through studies of collective oscillations [5,6], to the detailed analysis of in-trap density profiles [7–9]. However, regardless of which technique is used, all such measurements depend on accurate knowledge of the properties of the Feshbach resonance that is used to tune the interactions.

${}^6\text{Li}$  atoms in the three energetically lowest Zeeman sublevels of the electronic ground state (labeled |1>, |2> and |3> following Ref. [10]) are widely used to realize strongly interacting Fermi gases. The interactions between atoms in the three different spin states are described by three scattering lengths  $a_{12}$ ,  $a_{23}$ , and  $a_{13}$ , which can all be tuned using broad Feshbach resonances located at magnetic fields of about 800 G with resonance widths of up to 300 G [11]. These resonances have been used to create the

best-known realization of a Fermi gas with diverging scattering length, which is a valuable benchmark system for many-body theories. How well this benchmark system can be realized is currently limited by the accuracy of the previous determination of the resonance positions, which was  $\leq 1.5$  G [10]. Recent studies of the equation of state (EOS) of strongly interacting Fermi gases have reached a level of precision at which they are limited by these uncertainties in the resonance positions. An important example is measurements recently performed by Nascimbéne *et al.* [7] and Ku *et al.* [9] with the goal of measuring the EOS at the point where the scattering length diverges to  $\pm\infty$ . In this so-called unitary limit the scattering length drops out of the problem, leaving the interparticle spacing as the only remaining length scale. At zero temperature this has the consequence that all extensive quantities of the unitary Fermi gas are given by their values for a noninteracting system rescaled by a universal numerical constant  $\xi$  known as the Bertsch parameter [12]. Ku *et al.* determined this parameter to be  $\xi = 0.376 \pm 0.004$ , providing a precision measurement that can serve as a test for theories in such different fields as cold gases, nuclear physics, and the physics of neutron stars. However, if the measurement is performed at a finite value of the scattering length, it leads to systematic errors. The error in  $\xi$  resulting from the 1.5 G uncertainty in the resonance position determined by Bartenstein *et al.* is about 2% and is the largest error contribution [9]. This clearly illustrates the necessity of a new, more accurate determination of the properties of the  ${}^6\text{Li}$  Feshbach resonances.

In this work we determine the positions of the broad  ${}^6\text{Li}$  Feshbach resonances with an accuracy of 80 mG, which corresponds to less than  $7 \times 10^{-4}$  of the resonance widths. To achieve this, we make use of the fact that every Feshbach resonance is related to a weakly bound dimer state. Close to the resonance the binding energy of the dimer is approximately related to the scattering length by the universal relation  $E_b = \hbar^2/ma^2$ , where  $m$  is the mass of one atom [2]. Thus we can obtain information about the  ${}^6\text{Li}$  Feshbach resonances by measuring the binding energy of such a weakly bound dimer state for different values of the magnetic field. However, the universal relationship is not accurate enough for quantitative interpretation, and in the present work we fit the measured binding energies to determine a new model interaction potential for  ${}^6\text{Li}$  using coupled-channel calculations. This new potential in turn provides  $a(B)$  as a function of magnetic field  $B$  and allows us to characterize the Feshbach resonances to high precision.

The most precise method currently available to measure the binding energy of these dimers is RF spectroscopy [10,13]. This technique is based on applying an RF pulse to a gas of atoms to drive them from an initial hyperfine state  $|i\rangle$  to a final state  $|f\rangle$ . For a sample of molecules, one can either drive a transition to another weakly bound dimer state (bound-bound transition) or dissociate the dimer into two free atoms (bound-free transition). In either case, the transition frequency is shifted from the free-free transition by the difference in the binding energies of the initial and final states. However, the transition frequency is also affected by the difference in the mean-field energies of the initial and final states. To avoid this systematic error, measurements of the dimer binding energy must be performed in a regime where the scattering length is much smaller than the interparticle spacing, i.e.,  $na^3 \ll 1$ . In previous experiments this could be achieved only for relatively small values of  $a \lesssim 2000a_0$ , as the experimentally achievable densities were limited to  $n \gtrsim 10^{13}$  molecules/cm $^3$ . Accordingly, the smallest binding energies that could be measured were on the order of  $E_b \approx h \times 100$  kHz, which resulted in a large uncertainty in the fitted resonance position.

We use the techniques we have developed to prepare and detect few-particle systems [14] to create very dilute samples of molecules. This allows us to perform RF spectroscopy of dimers with much smaller binding energies and thus measure much closer to the resonance. We start from a small Bose-Einstein condensate of about  $10^3$   $|12\rangle$  molecules trapped in a small-volume optical dipole trap at a magnetic field of 760 G. Subsequently, we reduce the particle number to about 30 molecules by applying the spilling technique developed in Ref. [14]. We then superimpose a large-volume optical dipole trap with trap frequencies of  $\nu_r = \omega_r/2\pi = 349(3)$  Hz and  $\nu_{ax} = \omega_{ax}/2\pi = 35(1)$  Hz in the radial and axial directions, respectively. To transfer the molecules into this shallow dipole trap, we suddenly

switch off the microtrap. This nonadiabatic release results in a mean kinetic energy per particle of  $\geq 0.4 \mu\text{K}$  and therefore a final molecular peak density of  $n \leq 10^9$  molecules/cm $^3$ , which greatly reduces density-dependent shifts of the RF transition [15].

To measure the bound-free spectra, we first perform a 10 ms ramp from the magnetic field of 760 G at which we prepare the sample to the magnetic field of interest and wait for another 5 ms. This time is long enough for the magnetic offset field to stabilize to an uncertainty of typically 1 mG, but short enough to avoid collisional dissociation of a significant fraction of molecules. We then apply a rectangular RF pulse of 10 ms duration to dissociate a fraction of the  $|12\rangle$  molecules into free atoms in states  $|1\rangle$  and  $|3\rangle$ . By measuring the number of these unbound atoms as a function of the RF frequency, we obtain spectra as shown by blue dots in Fig. 1. To limit saturation effects, we choose the pulse power such that we dissociate at most 30% to 40% of the molecules.

To measure the frequency of the free-free transition, we prepare a spin-polarized Fermi gas of atoms in state  $|2\rangle$  and drive the RF transition to state  $|3\rangle$  (red dots in Fig. 1). We do this before and after the molecule dissociation measurement and use the weighted mean  $\nu_{ff}$  of the two measurements [15]. From this we can also determine the magnetic field using the Breit-Rabi formula.

The profile of the bound-free spectrum is determined by the overlap between the wave functions of the initial molecular state  $\psi_i$  and of the accessible final states  $\psi_f$  [16]. As the RF photons carry only negligible momentum, there is no net momentum transfer to the system, and therefore the RF pulse can affect only the relative motion of the two atoms. The transition rate between the initial and final state is thus proportional to  $|\langle \psi_i(r) | \psi_f(r) \rangle|^2$ , where  $r$  is the distance between the two atoms. For a continuum of final states the resulting asymmetric line shape is given by the momentum distribution of the initial molecular state [16]. In a confining potential, however, the final states are

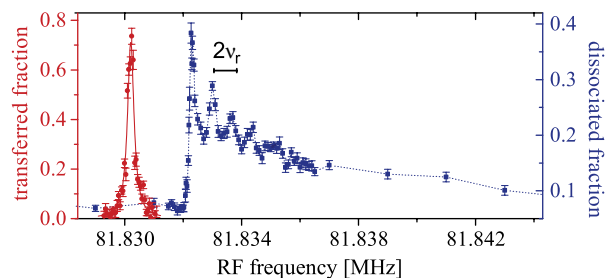


FIG. 1 (color online). RF spectra for the free-free (red dots, left axis) and bound-free (blue squares, right axis) spectra at a magnetic field of  $B = 811.139$  G. The line shape of the free-free transition is well described by a Lorentzian (solid line). The bound-free spectrum shows distinct peaks spaced by  $2\nu_r$ , corresponding to different radial trap levels. The errors are the standard errors of the mean of about 40 individual measurements.

the discrete energy levels of the trap, and the profile is determined by the overlap between the molecular state and the trap states. If the experimental resolution is insufficient to resolve the trap levels, as was the case in previous experiments [3,4,10,13], the final state can be well described by a continuum. In our case the resolution is high enough to resolve the radial trap levels (see Fig. 2).

For the initial molecular state, the long-range part of the wave function for the relative motion is well described by  $\psi_i(r) \simeq e^{-r/a}$ , where  $a$  is the scattering length. The final states are the levels of our optical trap, which we approximate as harmonic oscillator levels. Since the initial state is symmetric, only the symmetric harmonic oscillator levels ( $n_{\text{ho}} = 0, 2, 4, \dots$ ) contribute. Calculating the wave function overlap results in a spectrum of delta functions of different heights located at  $\nu_{\text{bf}} + p\nu_r + q\nu_{\text{ax}}$ , where  $\nu_{\text{bf}}$  is the frequency of the bound-free transition and  $p, q$  are non-negative even integers. To fit our measured spectra, we convolute this spectral function with the line shape of the free-free transition, which we approximate by a Lorentzian with a FWHM of 122 Hz. Because of this finite resolution, only the radial peaks are resolved. The free parameters of

the fits are  $\nu_{\text{bf}}$ , the overall amplitude, and a small offset in the atom number arising from collisional dissociation of molecules [17]. To determine  $\nu_{\text{bf}}$  we fit the lowest radial peak at each field (solid lines in Fig. 2) [18]. The molecular binding energies obtained by subtracting the confinement-induced frequency shifts [15,19] from the dissociation frequencies  $\nu_{\text{bf}} - \nu_{\text{ff}}$  are given in Table I.

To fit the experimental results and extract the position of the broad resonance pole, we use a coupled-channel model similar to that of Refs. [10,20]. The interaction potentials are constructed using the short-range singlet potential of Ref. [21] and the short-range triplet potential of Ref. [22] joined at long range onto potentials based on the dispersion coefficients of Ref. [23] and the exchange function of Ref. [21]. The interatomic spin-dipolar interaction is taken to follow its long-range ( $r^{-3}$ ) form at all distances. The singlet and triplet scattering lengths are adjusted by making small changes to the repulsive walls of the singlet and triplet potentials with parameters  $S_0$  and  $S_1$ . Scattering calculations are carried out using the MOLSCAT package [24] and bound-state calculations using the companion package BOUND [25,26]. MOLSCAT can converge directly on the positions of poles and zeroes in the scattering length. We carried out least-squares fits to the new binding energy measurements described above, together with the two bound-bound spectroscopic frequencies of Ref. [10] at 661.436 and 676.090 G, the magnetic field near 527 G where the scattering length passes through zero [27], and the position of the narrow resonance near 543 G [28]. The least-squares fits were carried out using the interactive package I-NoLLS [29].

A two-parameter fit using only  $S_0$  and  $S_1$  proved capable of giving a good fit to all the experimental results *except* the position of the narrow resonance. This fit placed the narrow resonance about 0.12 G to high field of its experimental position. This discrepancy could be resolved by introducing a third parameter in a variety of ways, such as scaling the exchange potential or changing the value of the exponent parameter  $\beta$  in the exchange potential. However, in the absence of a good theoretical justification for the extra parameters, and since introducing them had little effect on the parameters of the resonances near 800 G, we ultimately chose a two-parameter fit, excluding the data point for the pole of the narrow resonance, as the most reliable for our purpose. To estimate the uncertainties in the pole positions and derived parameters, we repeated the fits using binding energies at the upper and lower limits of the systematic uncertainties and used the range of predictions from the various fits to estimate the model dependence.

The quality of fit and the key quantities calculated from the best-fit (two-parameter) potential are summarized in Table II. Tabulations of  $a(B)$  for the best-fit potential are given in the Supplemental Material [15].

With these results, the uncertainty in the positions of the broad  ${}^6\text{Li}$  Feshbach resonances is no longer a limiting

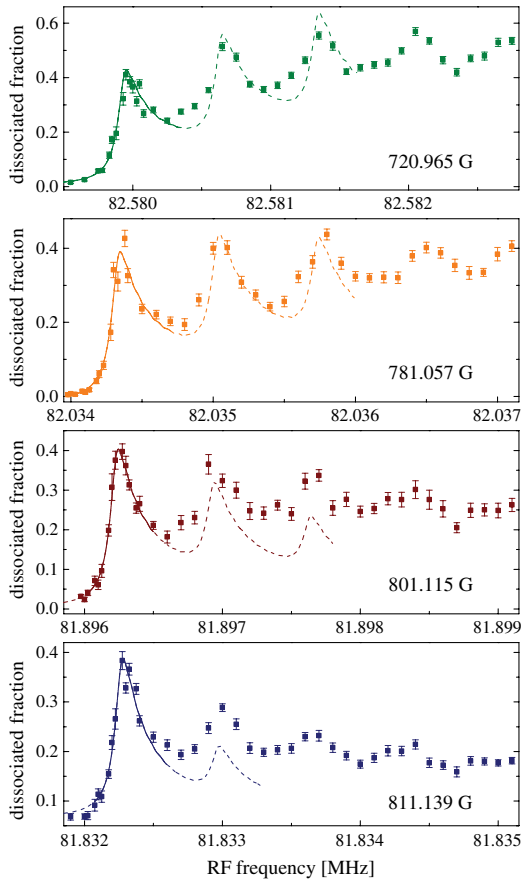


FIG. 2 (color online). Molecular dissociation spectra at four different magnetic fields. The lines show fits according to the model described in the text, with the solid parts indicating the range of the data points included in the fit.

TABLE I. Measured frequencies and resulting binding energies at different magnetic fields. The dissociation frequency  $\delta\nu$  is obtained by subtracting the free-free transition frequency  $\nu_{\text{ff}}$  from the bound-free transition frequency  $\nu_{\text{bf}}$ . To obtain the binding energy we subtract the confinement induced frequency shift  $\nu_{\text{cs}}$  from the dissociation frequency  $\delta\nu$ . The different contributions to the confinement induced shift  $\nu_{\text{cs}}$  and the statistical (stat.) and systematic (sys.) errors are discussed in the Supplemental Material [15].

Magnetic field $B$ (stat.) (G)	Free-free transition $\nu_{\text{ff}}$ (stat.) (MHz)	Bound-free transition $\nu_{\text{bf}}$ (stat.)(sys.) (MHz)	Dissociation frequency $\nu_{\text{bf}} - \nu_{\text{ff}}$ (stat.)(sys.) (kHz)	Confinement shift $\nu_{\text{cs}} = \nu_0(\text{sys.}) + \nu_i(\text{sys.})$ (kHz)	Binding energy/ $h$ $\nu_{E_b}$ (stat.)(sys.) (kHz)
811.139 (1)	81.830 115 (3)	81.832 271 (7)(8)	2.156 (8)(16)	0.367(3) – 0.014(1)	1.803 (8)(17)
801.115 (5)	81.891 539 (33)	81.896 236 (3)(8)	4.697 (33)(16)	0.367(3) – 0.011(1)	4.341 (33)(17)
781.057 (1)	82.019 823 (1)	82.034 336 (6)(8)	14.513 (6)(16)	0.367(3) – 0.011(1)	14.157 (7)(17)
720.965 (1)	82.452 482 (2)	82.579 943 (13)(8)	127.461 (13)(16)	0.367(3) – 0.021(1)	127.115 (14)(17)

factor for current experiments. Using our new calibration of  $a(B)$  it is possible to address systematic errors in recent experiments which were caused by the inaccuracy of the previous determination of the resonance positions. The most striking example of this is the determination of the Bertsch parameter  $\xi$  by Ku *et al.* [9], which was performed using a mixture of  ${}^6\text{Li}$  atoms in states  $|1\rangle$  and  $|2\rangle$  at a magnetic field of 834.15 G. At this field, our best-fit potential gives  $a(B) = -2.124(80) \times 10^5 a_0$  and effective range  $r_{\text{eff}} = 87.03(1)a_0$ . The difference between the EOS at unitarity and the EOS measured at this finite value of the scattering length may be obtained by using Tan’s contact  $C(a)$  [9,30]. This gives a corrected value for the normalized zero-temperature chemical

potential  $\mu/E_F$  at unitarity, which in turn gives a revised value of the Bertsch parameter  $\xi = 0.370(5)(8)$  [31]. Here the first parenthesis denotes the statistical error, while the second gives the systematic uncertainty of the corrected value [32].

In this work we have established a new technique to measure the binding energy of weakly bound molecules by performing trap-sideband-resolved RF spectroscopy. By creating very dilute samples of molecules we have greatly reduced density-dependent shifts of the RF transitions, which has allowed us to perform spectroscopy of extremely weakly bound molecules. Using these techniques we have measured the binding energy of  ${}^6\text{Li}$  Feshbach molecules with binding energies as low as  $h \times 2$  kHz with

TABLE II. Quality of fit between coupled-channel calculations on the best-fit two-parameter  ${}^6\text{Li}$  potential and the experiments, together with key derived quantities calculated using the potential. The quantities in parentheses are estimates of the model dependence, including the effect of the systematic errors in the binding energies in Table I. All frequencies are given in kHz, all lengths in bohr, and all magnetic fields in G. The  $\Delta$  and  $a_{\text{bg}}$  values are obtained from *local* fits to  $a(B)$  near the resonance and do not correctly reproduce the positions of the zeroes in  $a(B)$ .

	Fit Ref. [10]	Present fit	Experiment
$\nu_{b,12} - \nu_{b,13} + \nu_{\text{ff}}$ at 661.436 G	83 664.0(10)	83 665.9(3)	83 664.5(10) [10]
$\nu_{b,12} - \nu_{b,13} + \nu_{\text{ff}}$ at 676.090 G	83 297.3(10)	83 297.3(3)	83 296.6(10) [10]
$\nu_{b,12}$ at 720.965 G		127.115(17)	127.115(31)
$\nu_{b,12}$ at 781.057 G		14.103(26)	14.157(24)
$\nu_{b,12}$ at 801.115 G		4.342(17)	4.341(50)
$\nu_{b,12}$ at 811.139 G		1.828(11)	1.803(25)
Zero in $a_{12}$		527.32(25)	527.5(2)[27]
Narrow pole in $a_{12}$		543.41(12)	543.286(3)[28]
$a_s$	45.167(8)	45.154(10)	
$a_t$	-2140(18)	-2113(2)	

	Pole (G)		$\Delta$ (G)		$a_{\text{bg}}$ ( $a_0$ )	
	Ref. [10]	Present fit	Ref. [10]	Present fit	Ref. [10]	Present fit
12⟩	834.15	832.18(8)	300	-262.3(3)	-1405	-1582(1)
13⟩	690.43	689.68(8)	122.3	-166.6(3)	-1727	-1770(5)
23⟩	811.22	809.76(5)	222.3	-200.2(5)	-1490	-1642(5)

an accuracy better than  $h \times 50$  Hz, which is a 40-fold improvement compared to previous measurements [10]. From these binding energies we have determined the positions of the broad  ${}^6\text{Li}$  Feshbach resonances with an accuracy of 80 mG using a coupled-channels calculation. This removes one of the major limiting factors for precision studies of strongly interacting Fermi gases.

The authors thank M. Ku and M. Zwierlein for providing the corrected value of  $\xi$  as well as enlightening discussions. The authors gratefully acknowledge support from IMPRS-QD, Helmholtz Alliance HA216/EMMI, the Heidelberg Center for Quantum Dynamics, ERC Starting Grant No. 279697, EPSRC, AFSOR MURI Grant No. FA9550-09-1-0617, and EOARD Grant No. FA8655-10-1-3033.

\*lompe@physi.uni-heidelberg.de

†J.M.Hutson@durham.ac.uk

- [1] I. Bloch, J. Dalibard, and W. Zwerger, *Rev. Mod. Phys.* **80**, 885 (2008).
- [2] C. Chin, R. Grimm, P. Julienne, and E. Tiesinga, *Rev. Mod. Phys.* **82**, 1225 (2010).
- [3] C. Chin, M. Bartenstein, A. Altmeyer, S. Riedl, S. Jochim, J. Hecker Denschlag, and R. Grimm, *Science* **305**, 1128 (2004).
- [4] C. H. Schunck, Y. Shin, A. Schirotzek, and W. Ketterle, *Nature (London)* **454**, 739 (2008).
- [5] M. Bartenstein, A. Altmeyer, S. Riedl, S. Jochim, C. Chin, J. Hecker Denschlag, and R. Grimm, *Phys. Rev. Lett.* **92**, 203201 (2004).
- [6] J. Kinast, S. L. Hemmer, M. E. Gehm, A. Turlapov, and J. E. Thomas, *Phys. Rev. Lett.* **92**, 150402 (2004).
- [7] S. Nascimbène, N. Navon, K. J. Jiang, F. Chevy, and C. Salomon, *Nature (London)* **463**, 1057 (2010).
- [8] M. Horikoshi, S. Nakajima, M. Ueda, and T. Mukaiyama, *Science* **327**, 442 (2010).
- [9] M. J. H. Ku, A. T. Sommer, L. W. Cheuk, and M. W. Zwierlein, *Science* **335**, 563 (2012).
- [10] M. Bartenstein, A. Altmeyer, S. Riedl, R. Geursen, S. Jochim, C. Chin, J. Hecker Denschlag, R. Grimm, A. Simoni, E. Tiesinga *et al.*, *Phys. Rev. Lett.* **94**, 103201 (2005).
- [11] Units of gauss rather than Tesla, the accepted SI unit of magnetic field, are used in this paper to conform to the conventional usage of this field.
- [12] G. Baker, *Int. J. Mod. Phys. B* **15**, 1314 (2001).
- [13] C. A. Regal, C. Ticknor, J. L. Bohn, and D. S. Jin, *Nature (London)* **424**, 47 (2003).
- [14] F. Serwane, G. Zürn, T. Lompe, T. B. Ottenstein, A. N. Wenz, and S. Jochim, *Science* **332**, 336 (2011).
- [15] See Supplemental Material at <http://link.aps.org/supplemental/10.1103/PhysRevLett.110.135301> for details on the determination of the binding energy and for the table  $a(B)$  for the  $|12\rangle$ ,  $|13\rangle$ , and  $|23\rangle$  channels.
- [16] C. Chin and P. S. Julienne, *Phys. Rev. A* **71**, 012713 (2005).
- [17] C. Chin and R. Grimm, *Phys. Rev. A* **69**, 033612 (2004).
- [18] As we chose to dissociate a relatively large fraction of the molecules ( $\approx 40\%$  for the first peak) to obtain a good signal-to-noise ratio for this fit, the absolute height of the peaks is affected by saturation. If the different peaks have similar heights, as is the case at  $B = 781$  G, saturation affects them equally and the model shows quantitative agreement for all peaks. If the peak heights differ strongly the model shows only qualitative agreement for the peaks corresponding to final states with higher energy (dashed lines in Fig. 2).
- [19] Z. Idziaszek and T. Calarco, *Phys. Rev. A* **74**, 022712 (2006).
- [20] K. M. O'Hara, S. L. Hemmer, S. R. Granade, M. E. Gehm, J. E. Thomas, V. Venturi, E. Tiesinga, and C. J. Williams, *Phys. Rev. A* **66**, 041401(R) (2002).
- [21] R. Coté, A. Dalgarno, and M. J. Jamieson, *Phys. Rev. A* **50**, 399 (1994).
- [22] C. Linton, F. Martin, A. J. Ross, I. Russier, P. Crozet, A. Yiannopoulou, L. Li, and A. M. Lyyra, *J. Mol. Spectrosc.* **196**, 20 (1999).
- [23] Z. C. Yan, J. F. Babb, A. Dalgarno, and G. W. F. Drake, *Phys. Rev. A* **54**, 2824 (1996).
- [24] J. M. Hutson and S. Green, computer code MOLSCAT, 2011.
- [25] J. M. Hutson, computer code BOUND, 2011.
- [26] J. M. Hutson, E. Tiesinga, and P. S. Julienne, *Phys. Rev. A* **78**, 052703 (2008).
- [27] X. Du, L. Luo, B. Clancy, and J. E. Thomas, *Phys. Rev. Lett.* **101**, 150401 (2008).
- [28] E. L. Hazlett, Y. Zhang, R. W. Stites, and K. M. O'Hara, *Phys. Rev. Lett.* **108**, 045304 (2012).
- [29] M. M. Law and J. M. Hutson, *Comput. Phys. Commun.* **102**, 252 (1997).
- [30] S. Tan, *Ann. Phys. (N.Y.)* **323**, 2971 (2008).
- [31] M. Ku and M. W. Zwierlein (private communication).
- [32] This systematic uncertainty is estimated from the difference between the corrected values for the chemical potential  $\mu/E_F = 0.370$ , energy  $E/E_F = 0.362$ , and free energy  $F/E_F = 0.375$  of the unitary Fermi gas, which should all converge to  $\xi$  for  $T \rightarrow 0$ .